NASA TECHNICAL MEMORANDUM

NASA TM X-1313

NASA TM X-1313

EXPERIMENTAL INVESTIGATION OF LIQUID SLOSHING IN A SCALE-MODEL CENTAUR LIQUID-HYDROGEN TANK

by Irving E. Sumner, Raymond F. Lacovic, and Andrew J. Stofan

Lewis Research Center
Cleveland, Ohio

NATIONAL AERONAUTICS AND SPACE ADMINISTRATION • WASHINGTON, D. C. • NOVEMBER 1966

NASA TM X-1313

EXPERIMENTAL INVESTIGATION OF LIQUID SLOSHING IN A SCALE-MODEL CENTAUR LIQUID-HYDROGEN TANK

By Irving E. Sumner, Raymond F. Lacovic, and Andrew J. Stofan

Lewis Research Center
Cleveland, Ohio

NATIONAL AERONAUTICS AND SPACE ADMINISTRATION

For sale by the Clearinghouse for Federal Scientific and Technical Information
Springfield, Virginia 22151 – Price $2.00

EXPERIMENTAL INVESTIGATION OF LIQUID SLOSHING IN A SCALE-MODEL CENTAUR LIQUID-HYDROGEN TANK

by Irving E. Sumner, Raymond F. Lacovic, and Andrew J. Stofan

Lewis Research Center

SUMMARY

An experimental investigation of liquid sloshing in a 1/3.67-scale-model Centaur-stage liquid-hydrogen tank was conducted to determine the sloshing characteristics and slosh-damping effectiveness of the following ring-baffle configurations: (1) a flat-ring baffle, (2) a scale model of a preliminary baffle configuration for the Centaur liquid-hydrogen tank consisting of a channeled ring and 3 bracket supports, and (3) a scale model of the AC-8 baffle configuration consisting of a channeled ring, 12 equally spaced vertical baffles, 12 baffle stiffners, and 3 equally spaced bracket supports.

Experimental values of (1) the fundamental frequencies of the liquid oscillations and (2) the horizontal slosh forces and damping ratios (logarithmic decrements) occurring at the fundamental frequencies were obtained for both the unbaffled and the baffled tank configurations for a range of liquid levels above the top of the concave oblate spheroidal tank bottom. Experimental values of the frequencies, horizontal slosh forces, and damping ratios at the first two natural frequencies of the liquid oscillations were determined for liquid levels below the top of the concave oblate spheroidal tank bottom. The measurement of both the vertical and the horizontal slosh forces provided pendulum analogy parameters (pendulum-arm-length ratio, pendulum-mass ratio, and pendulum-arm - hinge-point-location ratio) that would effectively represent liquid sloshing in the unbaffled tank configuration. The results of this investigation are presented in terms of dimensionless parameters that are generally applicable to tanks of any size that have similar geometric configurations and in which the liquid surface interface remains relatively flat.

INTRODUCTION

Propellant sloshing is a potential source of disturbance critical to the stability of space vehicles. Oscillations of the propellant masses result from the lateral displace-

ment or angular rotation of the vehicle during the powered phase of the flight. Severe sloshing results when the propellant oscillations are coupled with one or more of the perturbations of vehicle motion at nearly the fundamental frequency of the contained propellant.

An analysis of the coast-phase of the two-burn Atlas-Centaur (AC-4) vehicle indicated that an instability problem had occurred. This problem resulted from a failure to settle the liquid hydrogen to an acceptable level at the time of venting. The high liquid level resulted in mixed phase flow at the vent exit which, on expanding, produced large impingement forces on the vehicle tank in excess of the capability of the attitude control system. Preliminary analysis indicated that, for future two-burn missions, the instability problem could be resolved by suppressing the liquid-hydrogen oscillations that may have contributed to the failure. For this purpose a slosh baffle was proposed. This baffle was to be located below the nominal coast-phase liquid surface at a position corresponding to a liquid-depth ratio of 0.590.

In order to determine the effectiveness of the proposed baffle, it was necessary to determine the fundamental frequencies of oscillation, the slosh forces, and the damping ratios for the unbaffled and the baffled Centaur liquid-hydrogen tank configurations. However, the results of previous experimental investigations (refs. 1 and 2) could not be applied with confidence to the baffled Centaur liquid-hydrogen tank configuration because (1) the proposed baffle location was relatively close to the bottom of the tank and (2) the shape of the tank bottom differed significantly from any shape utilized in previous experiments. In addition, the configuration of the proposed slosh baffle and supporting structure was also considerably different from those employed in previous experimental investigations.

An experimental investigation of liquid sloshing in a 1/3.67-scale-model Centaur-stage liquid-hydrogen tank was therefore conducted at the NASA Lewis Research Center. Experimental data were obtained over a range of liquid-depth ratios above the top of the concave oblate spheroidal tank bottom for the following configurations: (1) an unbaffled tank, (2) a baffled tank employing a flat-ring baffle, (3) a baffled tank employing a preliminary-design Centaur slosh baffle consisting of a channeled ring and 3 bracket supports, and (4) a baffled tank employing the final baffle design and basic supporting structure chosen for the AC-8 Centaur liquid-hydrogen tank (see appendix). The final baffle consisted of a channeled ring, 12 vertical baffles, and 12 baffle stiffners. The baffle was supported by 3 brackets below the baffle and by 3 rods from above the baffle. The experimental damping ratios obtained for the flat-ring baffle are compared with semiempirical predictions for flat-ring baffles by Miles (ref. 1) and Cole (ref. 3) to determine whether the relatively close proximity of the tank bottom influenced the slosh-damping characteristics of the baffle. A small amount of experimental data was obtained for an unbaffled tank to determine sloshing characteristics for liquid levels below the top of the concave

oblate spheroidal tank bottom. Experimental data were also obtained for an unbaffled tank to determine several pendulum analogy quantities that would effectively represent the liquid sloshing. The contained liquid was water in all cases. The results of the investigation are presented in terms of dimensionless parameters that are generally applicable to tanks of any size with similar geometric configurations where the liquid interface remains relatively flat.

SYMBOLS

a	ratio of baffle area to tank cross-sectional area for a baffle with no radial clearance, $(W/r)(2 - W/r)$
b	minor semiaxis of concave spheroidal tank bottom, ft
D	tank diameter, ft
d	distance that baffle is located below quiescent liquid free surface, ft
F_s	horizontal slosh force, lb
g	acceleration due to gravity, 32.174 ft/sec^2
h	height of liquid surface from concave oblate spheroidal tank bottom, ft
h_c	height of liquid surface in equivalent flat-bottom cylindrical tank, $h_c = h + \frac{1}{3} b$, ft
h_n	distance of pendulum mass above center of gravity of undisturbed liquid, ft
I_o	moment of inertia of fixed mass, slugs/ft^2
L_p	length of pendulum arm, ft
l_{cg}	distance from concave oblate spheroidal tank bottom to center of gravity of fixed mass, ft
l_p	distance from concave oblate spheroidal tank bottom to hinge-point location of pendulum arm, ft
M	external moment on tank produced by liquid sloshing, ft-lb
m_o	fixed or nonsloshing mass, slugs
m_p	pendulum or sloshing mass, slugs
m_t	total mass of liquid in tank at given liquid level, slugs
r	tank radius, ft
V_s	speed of sound in liquid, ft/sec
W	baffle width, ft
X_o	excitation amplitude, ft
γ_p	half-angle through which pendulum oscillates, rad

δ damping ratio (logarithmic decrement), $\ln[(F_s)_n/(F_s)_{n+1}]$

ϵ_o first root of $J_1'(\epsilon_n) = 0$, 1.841

η frequency parameter, $\omega_n\sqrt{r/g} = \sqrt{\epsilon_o \tanh\left(\frac{h_c}{r}\epsilon_o\right)}$

λ slosh force parameter, $F_s/\rho g D^3$

ξ wave height, ft

ρ liquid density, slugs/ft^3

ω_n natural frequency of liquid oscillations, rad/sec

ω_o excitation frequency of tank, rad/sec

Subscripts:

av average

n cycle number, 1, 2, 3 . . .

APPARATUS

Scale-Model Tank and Baffles

A 1/3.67-scale model (fig. 1) of the Centaur liquid-hydrogen tank, 32.7 inches in diameter, was fabricated from clear plastic. A 1/3.67-scale model of the preliminary-design Centaur liquid-hydrogen tank baffle, and also a flat-ring baffle (fig. 2(a)), were constructed of aluminum. Both baffles were 2.19 inches wide and were supported by

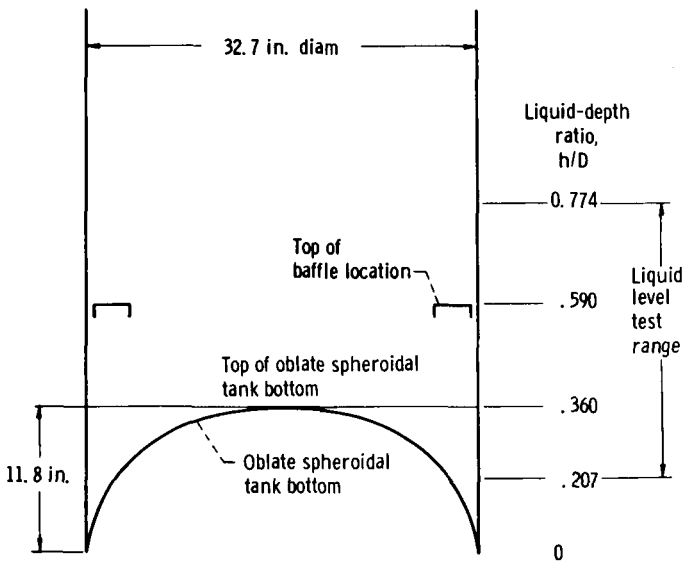

Figure 1. Schematic of scale-model Centaur liquid-hydrogen tank.

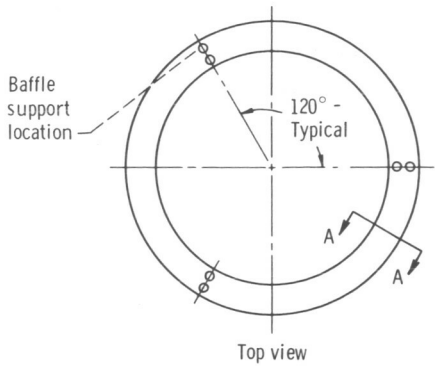

Preliminary-design Centaur baffle configuration	
Inside diameter, in.	28.06
Outside diameter, in.	32.44
Radial clearance from tank wall, in.	0.15
Baffle-width ratio, W/r	0.134
Cross-sectional area, $in.^2$	208.1

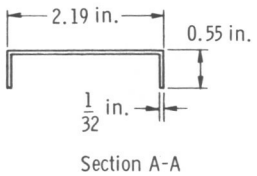

Section A-A

Flat ring baffle configuration	
Inside diameter, in.	28.35
Outside diameter, in.	32.72
Radial clearance from tank wall, in.	0
Baffle-width ratio, W/r	0.134
Cross-sectional area, $in.^2$	209.6

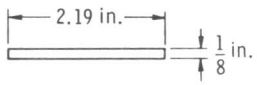

Section A-A

(a) Schematic view.

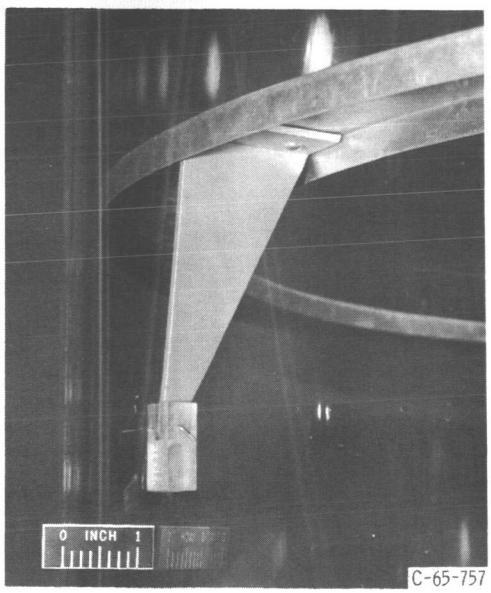

(b) Preliminary-design Centaur baffle configuration and support bracket.

Figure 2. - Scale-model baffle configurations.

three equally spaced scale-model aluminum brackets (fig. 2(b)). The preliminary-design Centaur scale-model baffle had a radial clearance of 0.15 inch from the tank wall; no radial clearance was provided for the flat-ring baffle. Both baffles were mounted at a liquid-depth ratio of 0.590 in the tank.

The scale-model AC-8 baffle configuration, which differed somewhat from the preliminary-design Centaur baffle configuration, is discussed in the appendix.

Experimental Test Facility

The experimental test facility, which is nearly identical to that described in references 4 and 5, is shown in figure 3. The scale-model Centaur liquid-hydrogen tank was mounted on a test bed that was suspended from a frame through three vertically oriented load cells and one horizontally oriented load cell. The frame was suspended from overhead crossbeams and was free to oscillate in one direction in the horizontal plane. The driving force was provided by a hydraulic piston and cylinder actuated by an electrically controlled servovalve. The excitation amplitude could be varied from 0 to 1 inch, and the excitation frequency could be varied from 0 to 20 cps. A sinusoidal excitation wave form was used for this investigation. The electric and hydraulic control circuits for the driving mechanism

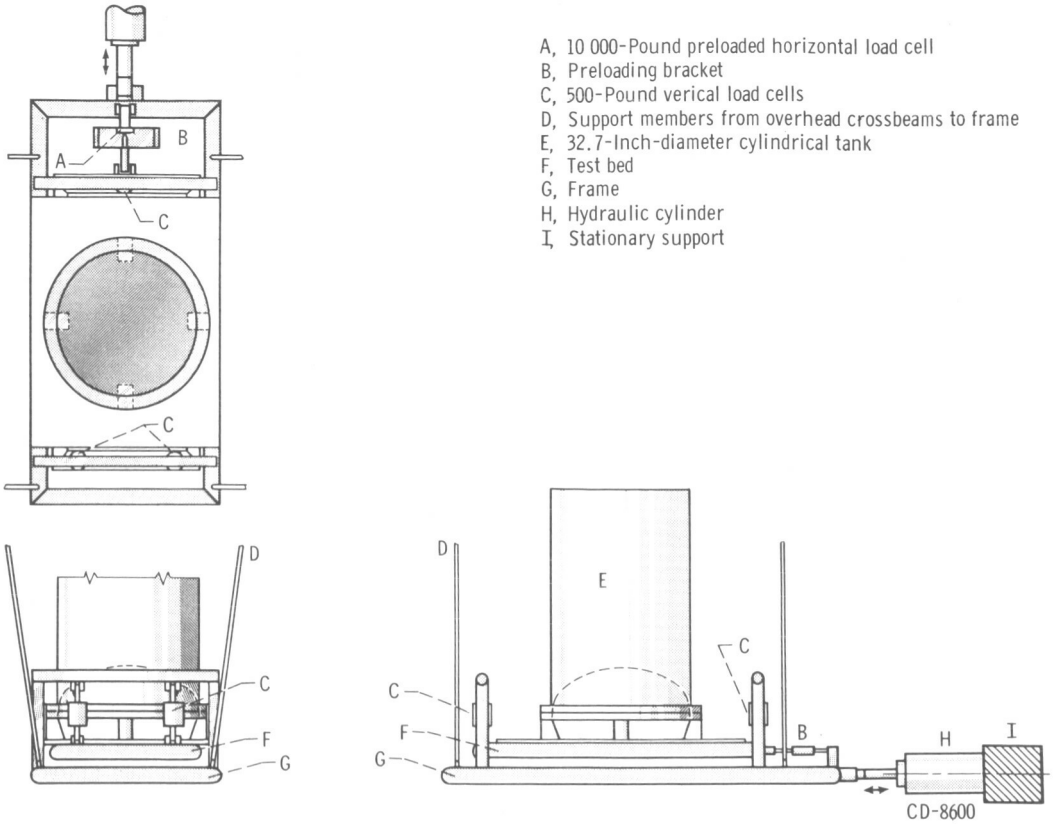

A, 10 000-Pound preloaded horizontal load cell
B, Preloading bracket
C, 500-Pound verical load cells
D, Support members from overhead crossbeams to frame
E, 32.7-Inch-diameter cylindrical tank
F, Test bed
G, Frame
H, Hydraulic cylinder
I, Stationary support

(a) Schematic view.

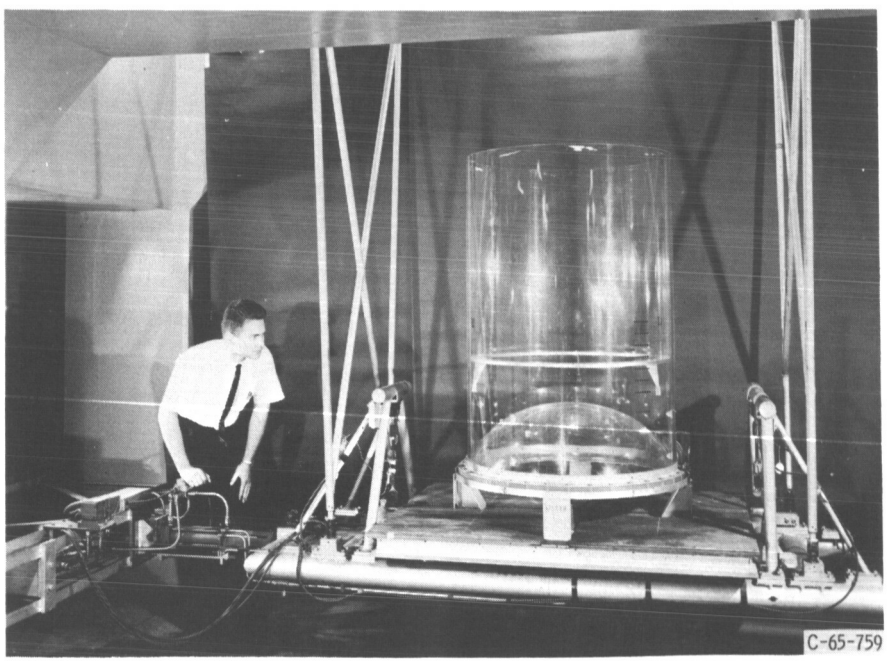

(b) Pictorial view.

Figure 3. - Experimental slosh-force test facility.

were designed to enable the oscillatory motion of the frame, test bed, and tank to be "quick-stopped" at a point of zero velocity during any given cycle of the oscillations so that only the residual forces resulting from the liquid sloshing could be measured. Water was the contained liquid in all cases.

The horizontal load cell was a piezoelectric quartz crystal that had been preloaded under compression. The vertical load cells were semiconductor transducers. The residual horizontal and vertical forces resulting from the liquid sloshing were sensed by the horizontal and vertical load cells, respectively, and the signals were displayed as continuously recorded oscillograph traces. The maximum error in obtaining the slosh forces from the oscillograph traces was approximately ±2.5 percent of the actual value.

PROCEDURE AND DATA REDUCTION

Liquid-Sloshing Characteristics

The tank was oscillated sinusoidally at a preselected excitation frequency (0.33 to 2.48 cps) and amplitude (0.017 to 0.399 in.). At each liquid-depth ratio, the excitation frequency chosen was equal to the actual fundamental frequency of the oscillations of the contained liquid. This selection provided the maximum slosh forces at a given excitation amplitude for liquid levels at or above the tank bottom. For liquid levels below the top of the concave tank bottom, the slosh forces occurring at the second natural frequency were also determined. When the waveform had built to its maximum height on the tank wall, the oscillation of the tank was quick-stopped, and the residual horizontal slosh forces were recorded on the oscillograph trace.

The first two natural frequencies of the liquid oscillations were determined by using the first several slosh-force peaks occurring immediately after the quick stop and were put into the form of the fundamental-frequency parameter $\eta = \omega_n \sqrt{r/g}$. The values of the horizontal slosh forces were determined by using the first slosh-force peak occurring immediately after the quick stop; the horizontal force was put into the form of the slosh-force parameter $\lambda = F_s/\rho g D^3$. The damping ratios were calculated from the logarithmic decrements $\delta = \ln\left(F_{s,n}/F_{s,n+1}\right)$ on each oscillograph trace. The fundamental frequencies, the slosh-force parameters, and the damping ratios were determined for both the unbaffled and the baffled tank configurations.

The maximum wave height of the liquid surface at the tank wall was determined for the flat-ring baffle at excitation frequencies and amplitudes corresponding to those for which the experimental slosh-force data had been obtained. The maximum wave heights were determined visually from two independent measurements by utilizing (1) a scale taped to the tank wall to measure wave height directly and (2) a protractor-type device to measure the slosh angle from the horizontal at which the liquid surface oscillated.

Quantities for Pendulum Analogy

Pendulum mass. - To obtain the quantities needed in calculating the pendulum mass (ref. 5), it was necessary to determine the horizontal slosh forces for steady-state conditions where the excitation frequency was less than the fundamental frequency of the contained liquid and was equal to the liquid oscillatory frequency. Excitation frequencies were varied from 40 to 75 percent of the fundamental frequency to determine the effect of a variation of excitation frequencies on the values obtained for the pendulum mass. The tank was oscillated at excitation amplitudes of 0.1 and 0.5 inch in order to drive the wave height of the liquid surface as high as possible, while the liquid surface still remained relatively flat. The slosh forces were thereby increased and their accuracy of measurement was improved. Once the wave height had reached a steady-state value, the oscillatory motion of the tank was quick-stopped, and the horizontal slosh forces were determined from the first force peak occurring immediately thereafter.

Hinge-point location. - The excitation frequency was equal to the fundamental frequency of the contained liquid. The excitation amplitude was varied from 0.017 to 0.075 inch depending on the liquid-depth ratio. The wave height was allowed to increase toward a maximum value with the following restrictions: (1) the liquid surface would remain relatively flat with no splashing of the contained liquid and (2) the liquid would be oscillating in exactly the same direction as the driving force (no swirl or rotary motion of the liquid surface). The oscillatory motion of the tank was then quick-stopped, and the residual forces resulting from the liquid sloshing were recorded. The vertical and horizontal slosh forces determined by using the first force peaks that occurred immediately after the quick stop were used to calculate the external moment M on the tank. The method of calculating the hinge-point location is presented in reference 5.

RESULTS AND DISCUSSION

Liquid-Sloshing Characteristics, Liquid-Depth Ratio $h/D \geq 0.360$

Fundamental-frequency parameter. - The fundamental-frequency parameter for liquid oscillations in the unbaffled scale-model Centaur liquid-hydrogen tank was initially calculated over a range of liquid levels above the top of the concave tank bottom ($h/D \geq 0.360$) by using an equivalent flat-bottom cylindrical-tank method (ref. 6):

$$\eta = \sqrt{\epsilon_o \tanh\left(\frac{h_c}{r}\epsilon_o\right)} \tag{1}$$

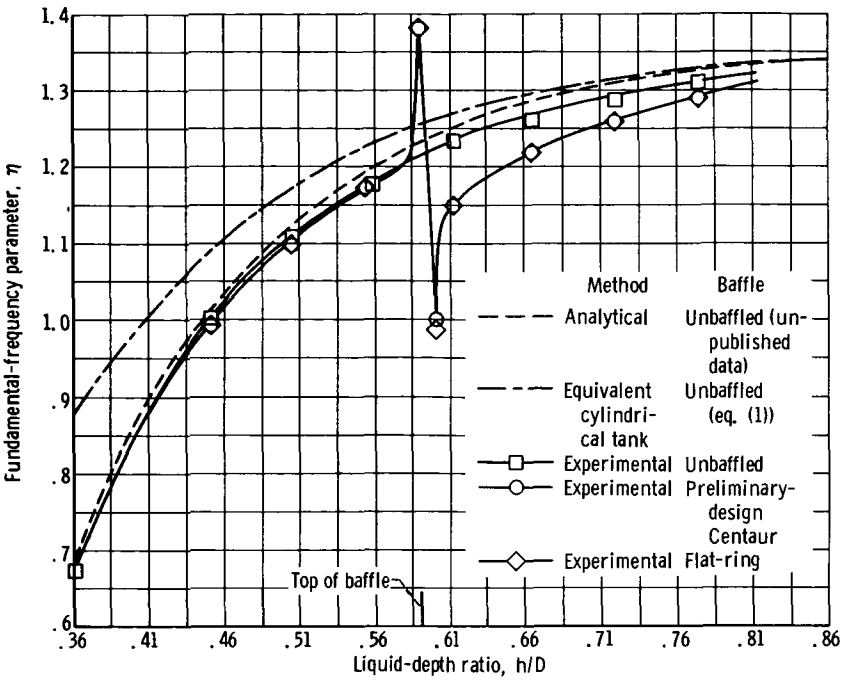

Figure 4. - Fundamental-frequency parameter for unbaffled and baffled tanks.

The fundamental frequencies for the unbaffled Centaur liquid-hydrogen tank were also predicted analytically for the exact tank configuration (unpublished data from General Dynamics/Convair) by using the hydrodynamic equations of liquid motion and the computer program for sloshing in rigid tanks (refs. 7 and 8). The equivalent flat-bottom cylindrical-tank method (eq. (1)), and analytical values are compared with experimentally determined values of the fundamental-frequency parameter $\eta = \omega_n \sqrt{r/g}$ for both the unbaffled and the baffled tank configurations (fig. 4). The results showed that, in general, the fundamental-frequency parameter increased with liquid-depth ratio until the concave bottom of the tank had little or no effect on the sloshing characteristics ($h/D > 0.860$) and approached the maximum value of 1.357 for high liquid levels in a cylindrical tank; that is, $\tanh\left[(h_c/r)\epsilon_o\right] = 1$.

The analytically determined frequency parameter compared more favorably with the experimental results than did the frequency parameter calculated by the equivalent flat-bottom cylindrical-tank method. The equivalent cylindrical-tank method is only an approximation, and the accuracy of the results may vary from one tank configuration to another. In this investigation where the concave tank bottom projected upward into the cylindrical tank, the value of the fundamental-frequency parameter was in error by 28 percent when the liquid level was at the top of the concave tank bottom ($h/D = 0.360$), but by 2 percent or less for values of $h/D > 0.660$.

The presence of either the Centaur baffle configuration or the flat-ring baffle configuration sharply increased the fundamental-frequency parameter when the liquid-depth

ratio corresponded to the baffle location and reduced the frequency parameter when the liquid level was slightly above the baffle location. Even though the flat-ring baffle had a slightly larger inside diameter and was mounted with no radial clearance between it and the tank wall, little or no difference in the values of the fundamental-frequency parameter for the two baffles was noted at a given liquid-depth ratio. Both baffles had the same baffle-width ratio ($W/r = 0.134$).

First-mode damping ratio. - Values of the damping ratio (logarithmic decrement) for liquid oscillations produced when the liquid was excited at its fundamental frequency were obtained for the unbaffled tank over a range of liquid-depth ratios for values of excitation amplitude parameter $0.00092 \leq X_o/D \leq 0.00305$. These data were obtained so that the increase in damping afforded by each baffle could be evaluated. The results (fig. 5) show that, generally, the damping ratios varied between values of $0.01 \leq \delta \leq 0.02$ for liquid-depth ratios $h/D > 0.460$. The damping ratios obtained for $X_o/D = 0.00305$ were somewhat higher because of ripples on the liquid surface due to a tendency of the liquid to splash from the tank walls. When the liquid level was near the tank bottom ($h/D < 0.460$), the damping ratios increased to $0.111 \leq \delta \leq 0.165$ because of the additional slosh damping afforded by the presence of the concave oblate spheroidal bottom.

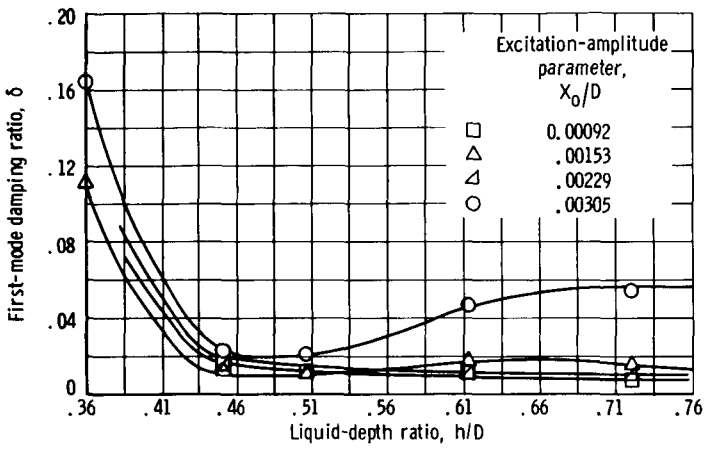

Figure 5. - First-mode damping ratio for unbaffled tank.

The first-mode damping ratios obtained over a range of liquid-depth ratios, $0.451 \leq h/D \leq 0.774$, with the preliminary-design Centaur baffle configuration mounted in the tank are presented in figure 6 for excitation-amplitude parameters $0.00052 \leq X_o/D \leq 0.00633$. Each data point represents the average damping for the first two oscillations of the liquid surface; generally, the damping ratio showed little variation for the first few cycles of the oscillations. The maximum damping occurred when the liquid surface was slightly above the baffle location (0.011 tank diam above top of baffle). The maximum values of the damping ratio increased from 0.30 to 0.64 as the excitation-amplitude parameter was increased; these values compare with damping ratios between approximately 0.01 to 0.06 obtained for the unbaffled tank.

The damping ratios obtained for the flat-ring baffle configuration are also presented in figure 6 for a range of liquid-depth ratios, $0.612 \leq h/D \leq 0.774$, to provide a basis for a comparison of the effectiveness of the preliminary-design Centaur baffle configuration.

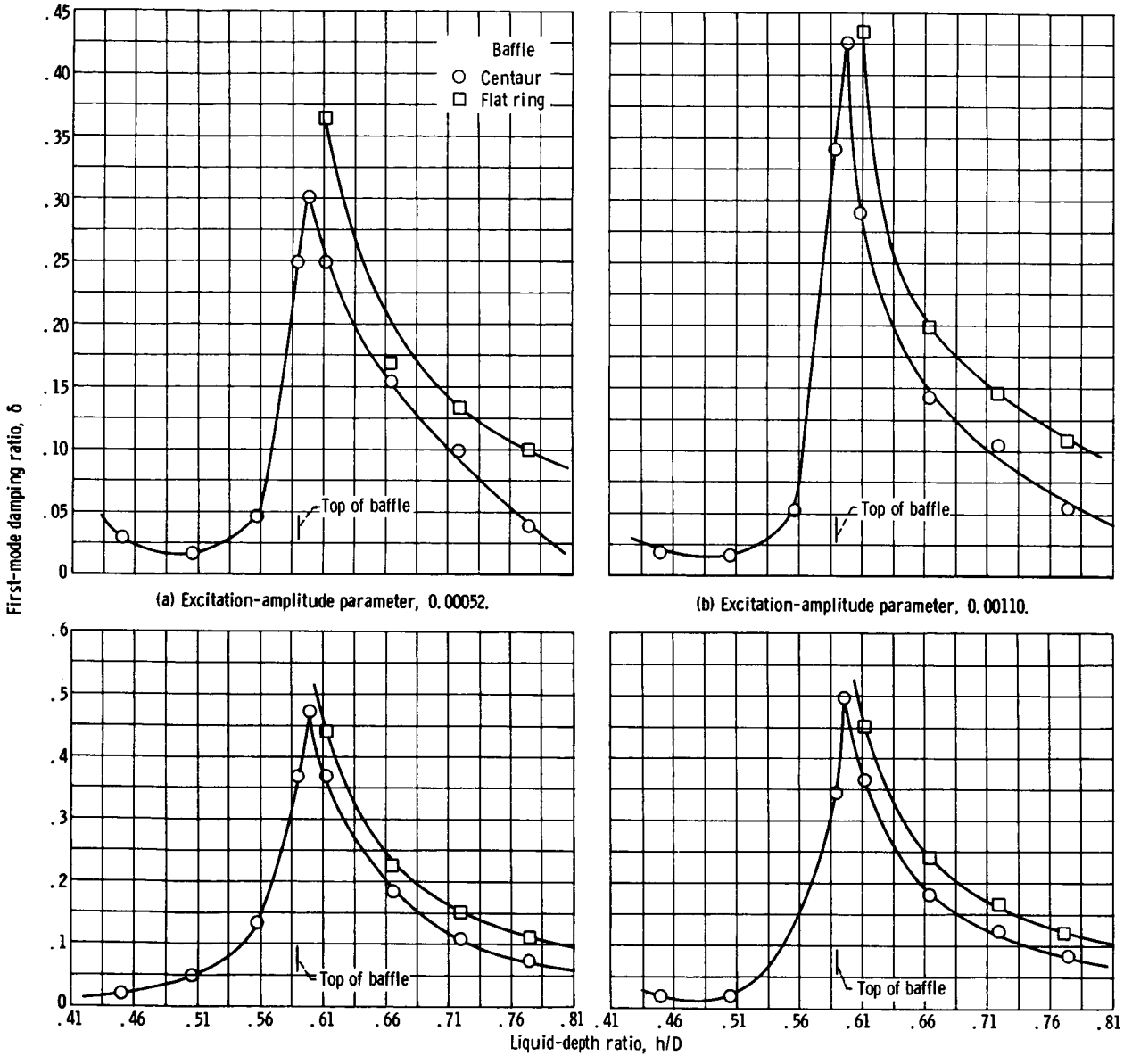

(a) Excitation-amplitude parameter, 0.00052.

(b) Excitation-amplitude parameter, 0.00110.

(c) Excitation-amplitude parameter, 0.00174.

(d) Excitation-amplitude parameter, 0.00235.

Figure 6. - First-mode damping ratio for baffled tank; flat-ring and preliminary-design Centaur baffle configurations.

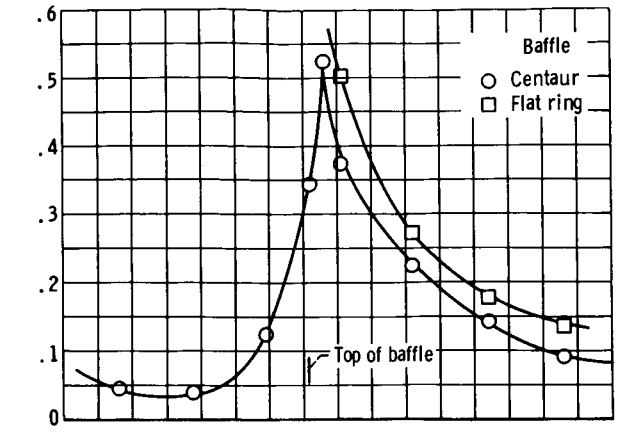

(e) Excitation-amplitude parameter, 0.00303.

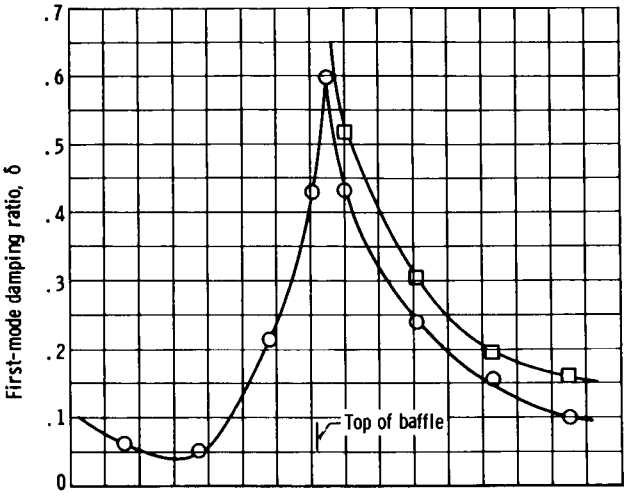

(f) Excitation-amplitude parameter, 0.00468.

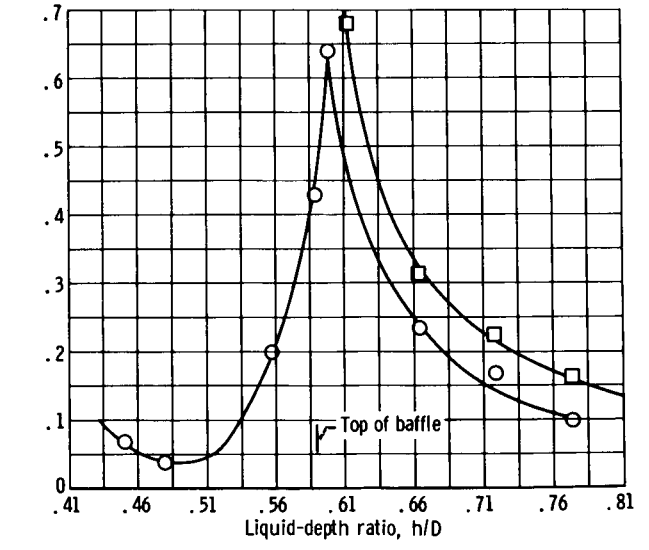

(g) Excitation-amplitude parameter, 0.00633.

Figure 6. - Concluded.

Each data point represents the damping for only the first cycle of oscillation of the liquid surface, since the damping ratio decreased rapidly from one cycle to the next for the first several cycles of the liquid oscillations. In all cases, the preliminary-design Centaur baffle configuration provided lower values of damping when compared with the flat-ring baffle. These lower values are attributed mainly to the radial clearance between the Centaur baffle and the tank wall, which reduced its slosh-damping effectiveness, even though both baffles had the same baffle-width ratio (W/r = 0.134). The fact that the two baffle configurations had slightly different cross-sectional areas (208.1 sq in. for the Centaur baffle compared with 209.6 sq in. for the flat-ring baffle) should afford a difference in damping of only about 1 percent (Miles damping equation, ref. 1).

The first-mode damping ratios which could be predicted for the flat-ring baffle were initially calculated using the Miles damping equation presented in reference 1:

$$\delta = 2\pi(2.83)e^{-4.6\,d/r}\,a^{3/2}\left(\frac{\xi}{r}\right)^{1/2} \tag{2}$$

A second equation proposed by Cole (ref. 3) to predict damping of the liquid oscillations was also utilized:

$$\delta = 2\pi(0.9)e^{-4.2\,d/r}\left(\frac{V_s^2}{rg}\right)^{1/8}\left(\frac{W}{r}\right)^{1.4}\left(1-\frac{W}{2r}\right)\left(\frac{\xi}{r}\right)^{0.35} \tag{3}$$

All the dimensionless parameters presented in equations (2) and (3) are functions of baffle and tank geometry with the exception of the ratio V_s^2/rg and the wave-height parameter ξ/r. The numerical value of the ratio V_s^2/rg was determined by using a value of 4800 feet per second for the velocity of sound in water.

The wave height of the liquid was visually determined by means of (1) a scale taped to the tank wall by which the wave height could be measured directly and (2) a protractor device by which the slosh angle of the liquid surface could be measured. Wave-height measurements were obtained for the flat-ring baffle over a range of excitation-amplitude parameters $0.00052 \le X_o/D \le 0.00633$ and liquid-depth ratios $0.612 \le h/D \le 0.774$. The liquid-sloshing conditions for the wave-height measurements corresponded to those for which the damping ratios were experimentally determined for the flat-ring baffle; the wave heights obtained were the maximum values for a given excitation amplitude and liquid-depth ratio. The results of the wave-height measurements (fig. 7) showed relatively good agreement between the two techniques of measurement.

The experimental values of the damping ratios obtained for the flat-ring baffle decreased rapidly from one cycle to the next for the first several cycles of liquid motion

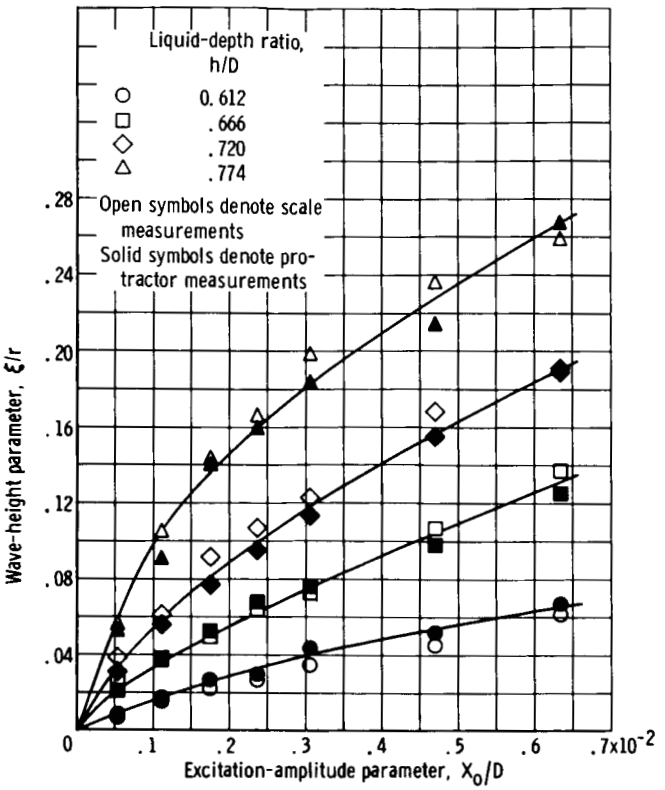

Figure 7. - Wave-height parameter for flat-ring baffle configuration.

occurring after the motion of the tank had been quick-stopped. Because the experimental damping ratios were evaluated by measuring the amplitude of the first two successive horizontal slosh-force peaks, it was desirable to use the average wave height corresponding to these two successive force peaks to calculate the expected damping ratio from equations (2) and (3). The average wave-height parameter $(\xi/r)_{av}$ corresponding to the first two successive slosh-force peaks was approximated by the following method:

(1) The wave height of the $n + 1$ liquid oscillation was determined from

$$\ln \frac{(F_s)_n}{(F_s)_{n+1}} = \delta \approx \ln \frac{\xi_n/r}{\xi_{n+1}/r} \tag{4}$$

(2) The average wave-height parameter was then assumed to be

$$\left(\frac{\xi}{r}\right)_{av} = \frac{\xi_n + \xi_{n+1}}{2r} \tag{5}$$

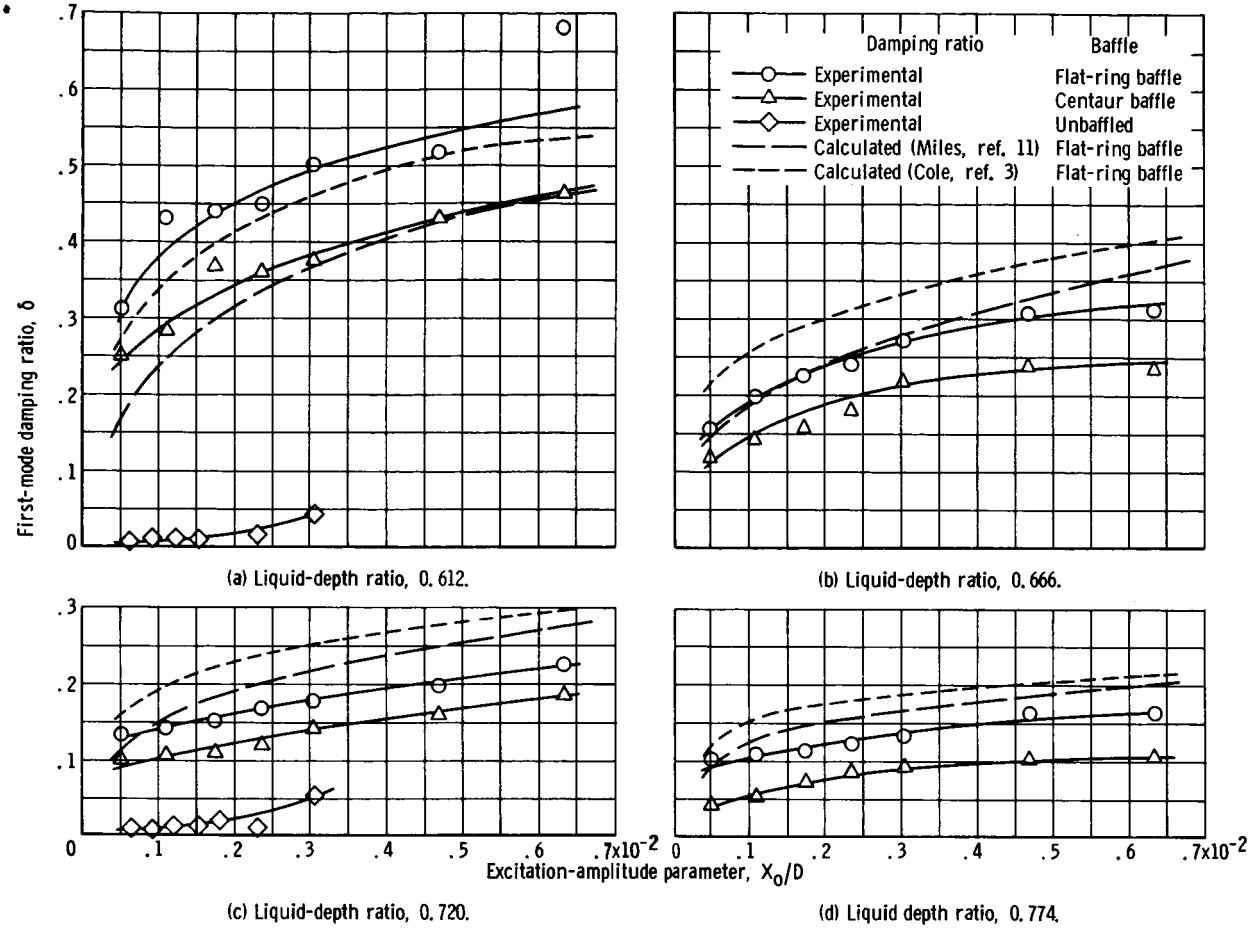

Figure 8. - Comparison of calculated and experimental first-mode dumping ratios.

The average wave-height parameter for only the first cycle of the liquid oscillation that occurred after the tank had been quick-stopped (n = 1) was used in equations (2) and (3) to predict the values of the first-mode damping ratio for the flat-ring baffle.

The first-mode damping ratios predicted by using equations (2) and (3) are compared with the experimental results for the flat-ring baffle in figure 8. These figures also compare the damping ratios of the preliminary-design Centaur baffle with those of the flat-ring baffle. Results for the unbaffled tank are also shown for two liquid-depth ratios. At a liquid-depth ratio of 0.612 (fig. 8(a)), the damping ratios predicted from the Cole damping equation shows reasonably good agreement with the experimental results obtained for the flat-ring baffle. The damping predicted for the flat-ring baffle from the Miles damping equation was less than the experimental values. This discrepancy apparently arises from the fact that at this liquid-depth ratio (h/D = 0.612), where the liquid level was only slightly above the baffle location, the liquid-free surface had a fairly complex wave shape, while the Miles damping equation assumes that the liquid surface remains smooth. The complex wave shape resulted in increased damping as also noted previously in

reference 9. In addition, the close proximity of the liquid surface to the concave bottom of the tank may also have provided some increase in the damping. The experimental results showed that the Centaur baffle configuration provided about 25 percent less damping than the flat-ring baffle but considerably more damping than for the unbaffled tank.

When the liquid level was increased to a liquid-depth ratio of 0.666 (fig. 8(b), p. 15), the Cole damping equation predicted damping ratios which were higher than the experimental values for the flat-ring baffle, while the Miles damping equation showed relatively good agreement at the lower values of the excitation amplitude parameter. This trend continued for the higher liquid-depth ratios investigated (figs. 8(c) and (d)) with the discrepancy between the values predicted by the Miles damping equation and the experimental values for the flat-ring baffle existing over a wider range of excitation-amplitude parameters at each higher liquid-depth ratio; however, this discrepancy never exceeded approximately 20 percent. In all cases, the Centaur baffle configuration provided about 25 percent less damping than the flat-ring baffle.

The differences, where they appear between the predicted and experimental damping ratios for the flat-ring baffle, are generally due to the restrictions placed on the applicability of both the Miles (ref. 10) and the Cole damping equations. These restrictions are as follows: (1) the maximum wave height must be small when compared with the tank radius, (2) the local flow in the regions near the baffle must not be affected by the presence of either the free surface or the bottom of the tank, and (3) the width of the baffle must be small when compared with the tank radius. Previous experimental investigations have shown that, within these restrictions, both equations (2) and (3) (p. 13) adequately predict values of damping for specific tank and baffle configurations (refs. 1, 3, and 9).

The experimental damping ratios for only a narrow flat-ring baffle ($W/r = 0.076$) for wave-height parameters less than 0.17 were compared with the predicted values of the Miles damping equation in reference 1. A wider baffle ($W/r = 0.157$) was utilized in reference 9; however, the baffle location was high enough in the tank ($h/D = 1.0$) that the bottom of the tank could not influence the sloshing characteristics to any appreciable extent. High values of the baffle-width parameter ($W/r = 0.083$ and 0.126) were also investigated in reference 3; however, the wave-height parameter was rather low ($\xi/r < 0.084$). For the tank and baffle configuration considered in this investigation, one or more of the restrictions noted appear to have been exceeded at some point in the test program when the range of liquid levels and wave heights utilized are considered. Therefore, adequate prediction of the damping provided by a flat-ring baffle from equations (2) and (3) could not have been reasonably expected over the entire range of all test variables investigated.

First-mode slosh-force parameter. - The variation of the first-mode slosh-force parameter with excitation-amplitude parameter is shown in figure 9 for the preliminary-design Centaur baffle and flat-ring baffle, as well as for the unbaffled tank, at a liquid-depth ratio of 0.612 ($h/D = 0.590$ for baffle location). The large reduction in the slosh-

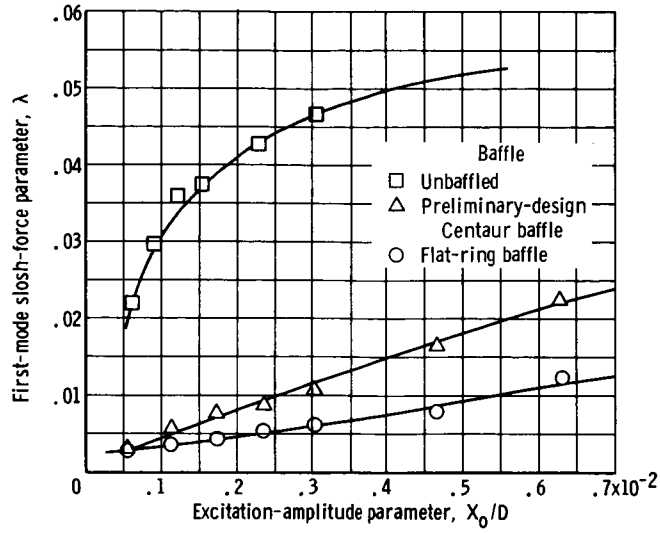

Figure 9. - Comparison of experimental first-mode slosh-force parameters for baffled and unbaffled tanks. Liquid-depth ratio, 0.612.

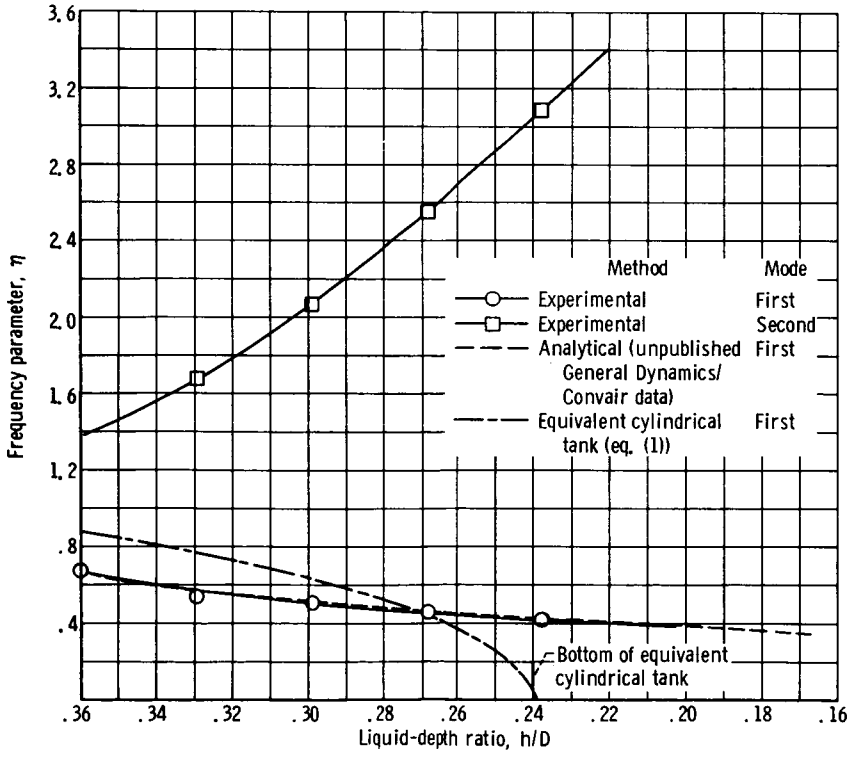

Figure 10. - First- and second-mode frequency parameters for liquid levels below top of concave oblate spheroidal tank bottom.

force parameter provided by either baffle as compared with the unbaffled tank is evident. The flat-ring baffle was more effective than the Centaur baffle in reducing the slosh forces due to the radial clearance that existed between the Centaur baffle and the tank wall.

Liquid-Sloshing Characteristics, Liquid-Depth Ratio $h/D \leq 0.360$

First- and second-mode frequency parameters. - The frequency parameters for the fundamental mode as well as the second natural mode of the liquid oscillations are presented in figure 10 (p. 17) for liquid depths below the top of the concave oblate spheroidal tank bottom ($h/D \leq 0.360$) (fig. 1, p. 4). The experimental and analytical values (unpublished data from General Dynamics/Convair) of the fundamental frequency parameters were in excellent agreement throughout the range of liquid-depth ratios investigated. The values of the fundamental frequency parameter calculated for the equivalent flat-bottom cylindrical tank (eq. (1)) did not show good agreement with the experimental and analytical values and could be calculated only to a liquid-depth ratio of 0.240, which represented the bottom of the equivalent cylindrical tank.

The second-mode frequency parameter increased as the liquid-depth ratio decreased, because the liquid was contained in an essentially toroidal or annular-shaped tank. As the liquid level decreases, therefore, the ratio of the inside to the outside radii of the annular section increases, and the second-mode natural frequency would also then be expected to increase (ref. 11).

First- and second-mode damping ratios. - The damping ratios obtained for the fundamental mode are shown in figure 11(a). As the liquid level decreased, the damping ratios decreased to minimum values at liquid-depth ratios $0.330 \geq h/D \geq 0.300$ and then increased because of the different flow paths of the liquid at varying depth ratios. When the liquid level was near the top of the concave oblate spheroidal tank bottom, the portion of the liquid near the surface tended to oscillate circumferentially over the concave oblate spheroidal tank bottom which provided a relatively large amount of damping. When the liquid level was well below the liquid-depth ratio of 0.360, the liquid tended to move circumferentially around the tank wall, which also provided a relatively large amount of damping. The minimum damping of the liquid oscillations was obtained at some intermediate liquid level between these two sloshing conditions. In all cases, the first mode damping ratios were approximately an order of magnitude greater than the damping ratios for the unbaffled tank at liquid-depth ratios well above the tank bottom ($h/D > 0.460$).

The second-natural-mode damping ratios increased to maximum values at a liquid-depth ratio of 0.300 and then decreased as the liquid level decreased (fig. 11(b)). This behavior, again, was due to the presence of the concave tank bottom, which influenced the amplitude of the liquid motion. Higher damping ratios were generally obtained at the liquid levels where the greater liquid motion occurred.

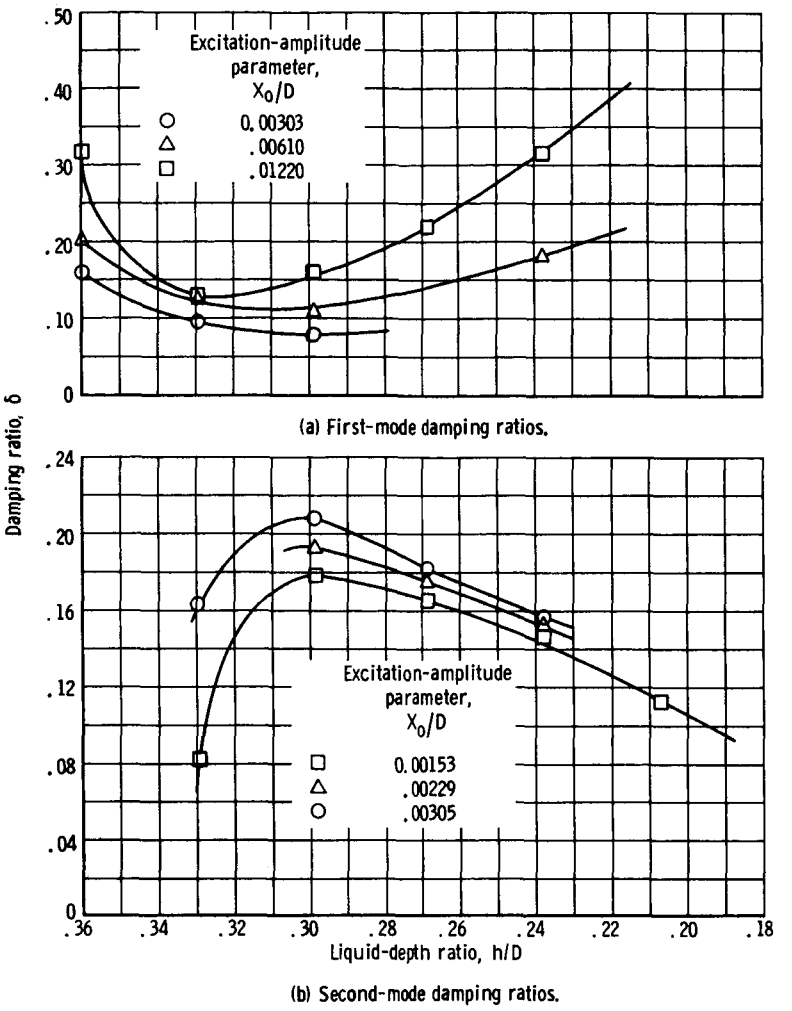

Figure 11. - Damping ratios for liquid levels below top of concave oblate spheroidal tank bottom.

First- and second-mode slosh-force parameters. - The first-mode slosh-force parameter decreased with a decrease in the liquid level (fig. 12(a), p. 20). Relatively high excitation amplitudes were required to provide any appreciable amount of liquid motion. The resulting slosh forces were approximately an order of magnitude less than the slosh forces produced at liquid-depth ratios well above the tank bottom ($h/D > 0.460$).

The second-mode slosh-force parameters increased to maximum values at liquid-depth ratios $0.300 \geq h/D \geq 0.270$ and then decreased as the liquid level decreased (fig. 12(b)). The maximum second-mode slosh-force parameters generally occurred at approximately the same liquid-depth ratios as the maximum damping occurred (fig. 11(b)).

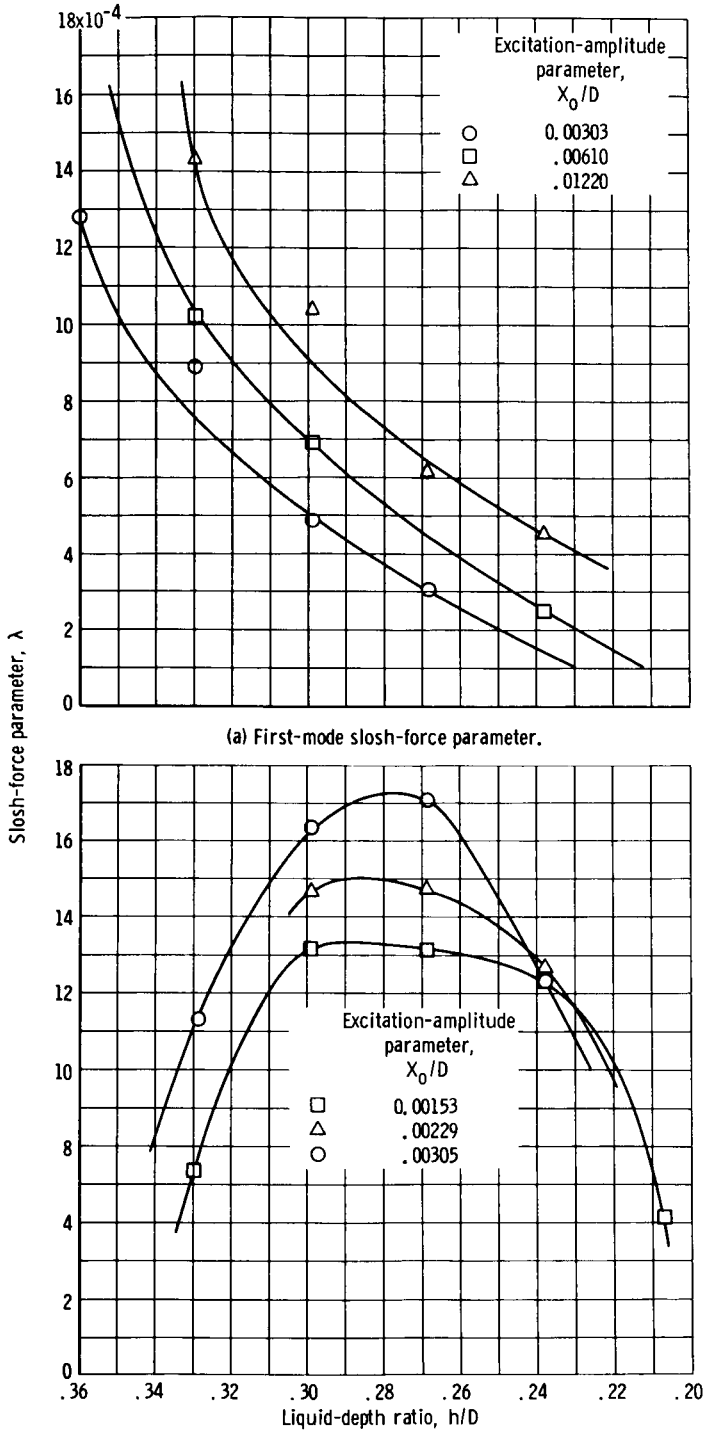

(a) First-mode slosh-force parameter.

(b) Second-mode slosh-force parameter.

Figure 12. - Slosh-force parameters for liquid levels below top of concave oblate spheroidal tank bottom.

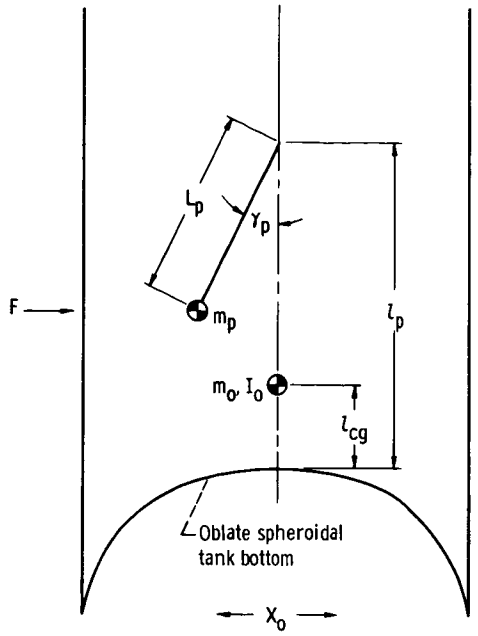

F force restraining horizontal motion of tank in test facility, equal to slosh force
I_o moment of inertia of fixed mass
L_p length of pendulum arm
l_{cg} distance from top of concave oblate spheroidal tank bottom to centroid fixed mass
l_p distance from top of concave oblate spheroidal tank bottom to pendulum-hinge point
m_p pendulum mass
m_o fixed mass
X_o excitation amplitude
γ_p half angle from vertical through which pendulum mass oscillates

Figure 13. - Quantities used to describe pendulum analogy of liquid sloshing for fundamental mode.

Pendulum Analogy Parameters, Liquid-Depth Ratio $h/D \geq 0.360$

The quantities necessary to represent the fundamental mode of liquid sloshing as mechanical pendulum analogy systems are presented in figure 13. Numerical values for the maximum half-angles γ_p through which the pendulum mass oscillates can be determined from figure 7 (p. 14), since previous experiments have shown that the pendulum arm remains normal to the liquid surface (ref. 12). Numerical values for the sloshing or pendulum mass m_p, the length of the pendulum arm L_p, and the location of the hinge-point location of the pendulum arm l_p were determined experimentally for the unbaffled tank by the techniques presented in references 5 and 12. These results are presented herein as dimensionless parameters and are compared with analytical results obtained (1) by using an equivalent flat-bottom cylindrical tank (ref. 13) and (2) by solving the hydrodynamic equations of liquid motion for the actual Centaur liquid-hydrogen tank configuration (unpublished data from General Dynamics/Convair).

The experimental values for the sloshing or pendulum mass were determined from (refs. 5 and 12)

$$m_p = \frac{F_s}{X_o}\left(\frac{1}{\omega_o^2} - \frac{1}{\omega_n^2}\right) \tag{5}$$

The calculated values for an equivalent flat-bottom cylindrical tank were determined from (ref. 13)

$$m_p = m_t \left[\frac{2 \tanh\left(\epsilon_o \frac{h_c}{r}\right)}{\left(\epsilon_o \frac{h_c}{r}\right)\left(\epsilon_o^2 - 1\right)} \right] \tag{6}$$

The experimental, the equivalent flat-bottom cylindrical tank, and the analytical (unpublished data, General Dynamics/Convair) values of the pendulum-mass ratio m_p/m_t are presented in figure 14. The experimental and analytical values of m_p/m_t increased, reached a maximum value of approximately 0.6, and then decreased as the liquid-depth ratio increased. The experimental and analytical values showed relatively good agreement over the entire range of the liquid-depth ratios investigated. The equivalent cylindrical-tank method indicated only a decrease in the values of m_p/m_t with an increase in the liquid-depth ratio and showed relatively good agreement with values obtained by the experimental and analytical programs only at the higher liquid-depth ratios where the concave bottom of the tank had little effect on the sloshing characteristics.

The length of the pendulum arm L_p may be calculated directly from the pendulum fundamental-frequency expression $L_p = g/\omega_n^2$. The dimensionless pendulum-arm-

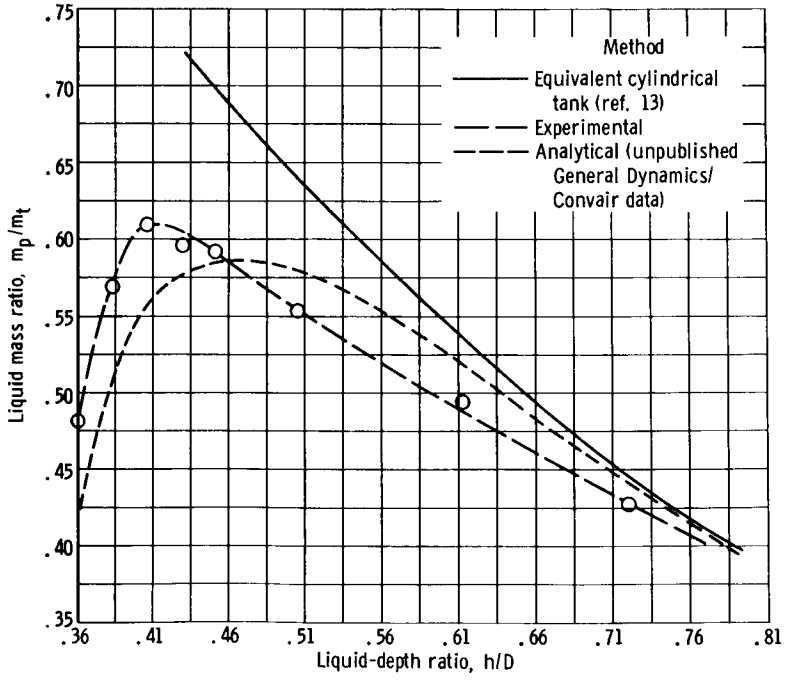

Figure 14. - Pendulum- or liquid-sloshing-mass ratio for unbaffled tank.

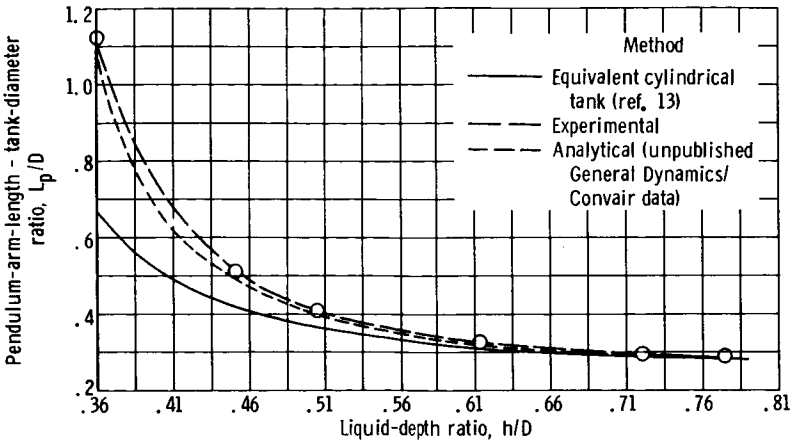

Figure 15. - Pendulum-arm-length ratio for unbaffled tank.

length - tank-diameter ratio $L_p/D = 1/2\eta^2$ is presented in figure 15 for a range of liquid-depth ratios $0.360 \leq h/D \leq 0.774$. The pendulum-arm-length - tank-diameter ratio decreased with an increase in the liquid-depth ratio. The experimentally determined values were in close agreement with the analytical values obtained from the unpublished, General Dynamics/Convair data over the entire range of liquid-depth ratios investigated. However, the ratios calculated by using the equivalent flat-bottom cylindrical-tank method showed good agreement with the experimental values only at the higher liquid-depth ratios $h/D > 0.510$ where the fundamental frequencies for the equivalent cylindrical tank (eq. (1)) were in close agreement with the experimentally obtained values (fig. 4, p. 9).

The experimental values of the hinge-point location were determined from $l_p = M/F_s$ (refs. 5 and 12). The calculated values for an equivalent flat-bottom cylindrical tank were determined from the following equation (ref. 13):

$$h_n = \frac{1}{2} h_c \left[1 - \frac{4}{\epsilon_o \frac{h_c}{r}} \tanh\left(\frac{\epsilon_o}{2} \frac{h_c}{r} \right) \right] \tag{7}$$

where h_n is the distance of the pendulum mass above the center of gravity of the undisturbed liquid or fixed mass. The distance to the center of gravity of the fixed mass (determined by using eq. (6)) above the bottom of the tank and the length of the pendulum arm (determined from the fundamental frequency calculated for the equivalent cylindrical tank) must be added to the value of h_n to obtain the hinge-point location above the bottom of the tank. A comparison of the experimental, calculated, and analytical values (unpublished data from General Dynamics/Convair) of the hinge-point-location ratio l_p/D presented in figure 16 indicates that the experimentally determined hinge-point location was

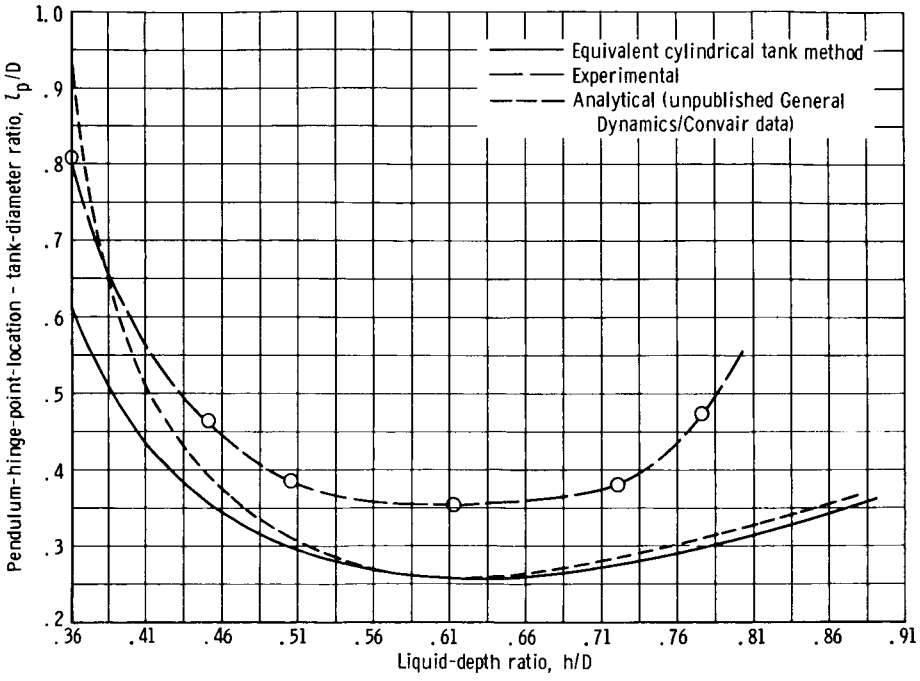

Figure 16. - Pendulum-hinge-point-location ratio for unbaffled tank.

generally higher in the tank than that predicted by either of the other methods over the entire range of liquid-depth ratios investigated. This result, again, appears to be due, in part, to the influence of the concave bottom of the tank on the sloshing characteristics.

SUMMARY OF RESULTS

An experimental investigation was conducted for unbaffled and baffled configurations of a 1/3.67-scale-model Centaur liquid-hydrogen tank to determine (1) the liquid-sloshing characteristics for liquid levels above and below the top of the concave oblate spheroidal tank bottom, (2) the slosh-damping effectiveness of a preliminary-design Centaur slosh baffle, consisting of a channeled ring and 3 bracket supports, compared with that of a flat-ring baffle, and (3) some of the quantities necessary to represent effectively liquid sloshing in the unbaffled tank configuration with a pendulum analogy. The following results are presented in terms of dimensionless parameters that are applicable to tanks of any size with similar geometric configurations where the liquid interface remains relatively flat:

1. The equivalent cylindrical tank method of predicting the fundamental frequency parameter for the unbaffled tank was adequate only for liquid-depth ratios greater than 0.660 where the error was 2 percent or less; the error at a liquid-depth ratio of 0.360 was 28 percent. The analytical method of predicting the fundamental frequency parameter from hydrodynamic equations of liquid motion showed good agreement with the experi-

mental results throughout the range of liquid levels investigated. When compared with the results obtained for the unbaffled tank, the presence of either the proposed Centaur slosh-baffle configuration or the flat-ring baffle (1) increased the fundamental frequency parameter when the liquid-depth ratio was equal to that of the baffle location and (2) reduced the frequency parameter when the liquid level was slightly above the baffle location.

2. The maximum damping ratios for the preliminary-design Centaur slosh-baffle configuration, obtained when the liquid level was 0.01 tank diameter above the baffle location, varied from 0.30 to 0.64 (compared with values of 0.01 to 0.06 for the unbaffled tank). The Centaur baffle configuration provided about 25 percent less damping than the flat-ring baffle. Calculated damping ratios obtained from the Miles damping equation (using experimentally determined wave heights) compared favorably with the damping ratios obtained for the flat-ring baffle only for (1) liquid levels well above the baffle location and (2) small values of the excitation-amplitude parameter. Experimental results indicate that the accurate prediction of liquid damping utilizing wave-height measurements becomes more difficult as the wave-height parameter is increased, and the baffle location approaches the bottom of the tank.

3. The values of the slosh-force parameter obtained for the flat-ring baffle were somewhat lower than those obtained for the Centaur slosh-baffle configurations. Both baffles provided considerable slosh-force suppression when compared with the results for the unbaffled tank. The decreased slosh damping and slosh-force suppression effectiveness of the proposed Centaur slosh-baffle configuration when compared with the flat-ring baffle is attributed mainly to the radial clearance which existed between the Centaur baffle and the tank wall. Liquid-sloshing characteristics were also determined for liquid levels below the top of the concave oblate spheroidal tank bottom.

4. Several pendulum analogy parameters (pendulum-mass ratio, pendulum-arm-length ratio, and pendulum-arm - hinge-point-location ratio) were determined experimentally for the unbaffled tank configuration. The experimental results were compared with values calculated from analytical methods by using the hydrodynamic equation of liquid motion and also from an equivalent flat-bottom cylindrical tank method. The experimental results showed good agreement with the analytical values (except for the hinge-point-location parameter) throughout a range of liquid levels above the tank bottom ($0.360 \leq h/D \leq 0.774$, where h/D is the liquid-depth ratio); the analytical values for the hinge-point-location parameter were generally less than those obtained experimentally. The pendulum analogy parameters calculated by the equivalent cylindrical

tank method showed poor agreement with the experimental results until the liquid level in the tank was high enough that the bottom of the tank no longer had an appreciable effect on the sloshing characteristics.

Lewis Research Center,
National Aeronautics and Space Administration,
Cleveland, Ohio, July 7, 1966,
891-01-00-06-22.

APPENDIX - AC-8 LIQUID-HYDROGEN TANK BAFFLE TESTS

The baffle configuration for the Atlas-Centaur AC-8 vehicle was similar to the preliminary-design Centaur liquid-hydrogen tank baffle configuration previously described except for the following additional equipment which had been installed:

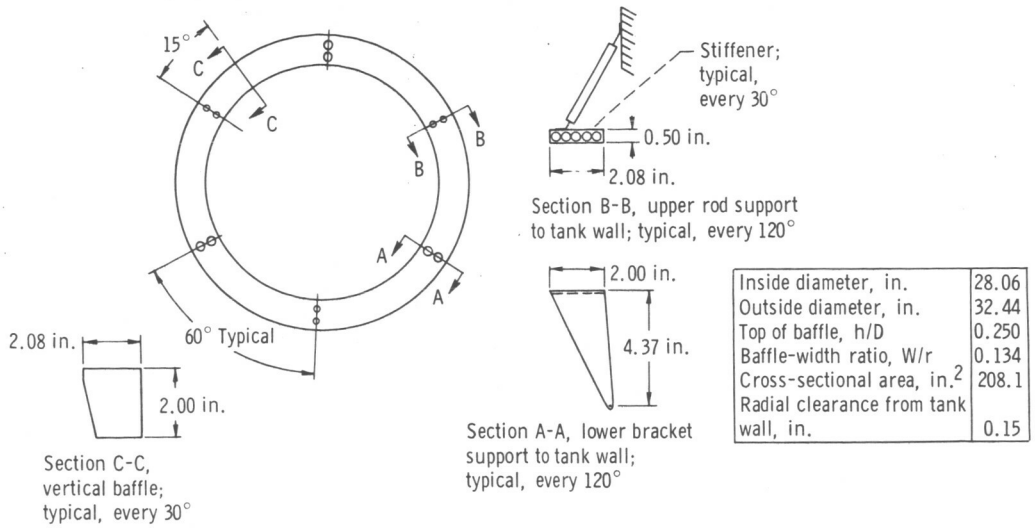

Inside diameter, in.	28.06
Outside diameter, in.	32.44
Top of baffle, h/D	0.250
Baffle-width ratio, W/r	0.134
Cross-sectional area, $in.^2$	208.1
Radial clearance from tank wall, in.	0.15

(a) Schematic view.

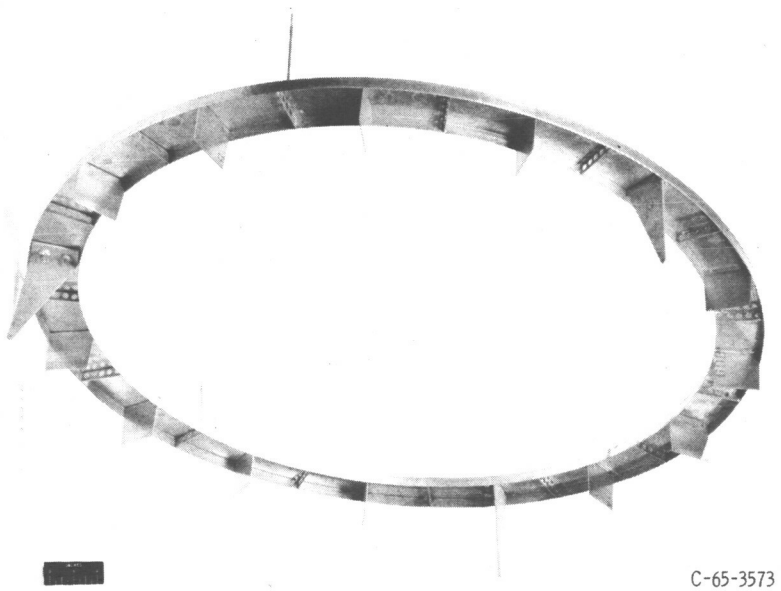

C-65-3573

(b) Pictorial view.

Figure 17. - Scale-model AC-8 baffle configuration.

(1) Three upper baffle supports located midway between the lower baffle supports every 120°

(2) Twelve vertical baffles located every 30° to damp any liquid swirling motion

(3) Twelve stiffners located every 30°

The scale-model baffle fabricated for this investigation is shown in figure 17. In addition, the AC-8 baffle was located somewhat higher in the tank (h/D = 0.610) than the baffle previously tested (h/D = 0.590). Therefore, it was necessary to perform additional experimental tests to determine the slosh damping characteristics for this particular baffle configuration.

The variation of the fundamental frequency parameter with liquid-depth ratio for the AC-8 baffle configuration (fig. 18) was similar to that observed for the previous baffle configuration (fig. 4, p. 9). The frequency parameters corresponded to that for an unbaffled tank when the liquid level was well below the baffle location. The presence of the AC-8 baffle configuration increased the frequency parameter when the liquid surface was in the immediate vicinity of the baffle and decreased the frequency parameter when the liquid level was slightly above the baffle location. The frequency parameter again approached the values for an unbaffled tank when the liquid level was well above the baffle location (h/D > 0.710).

The maximum first-mode damping ratios provided by the AC-8 baffle configuration occurred at liquid levels 0.01 tank diameter above the top of the baffle (fig. 19) and were

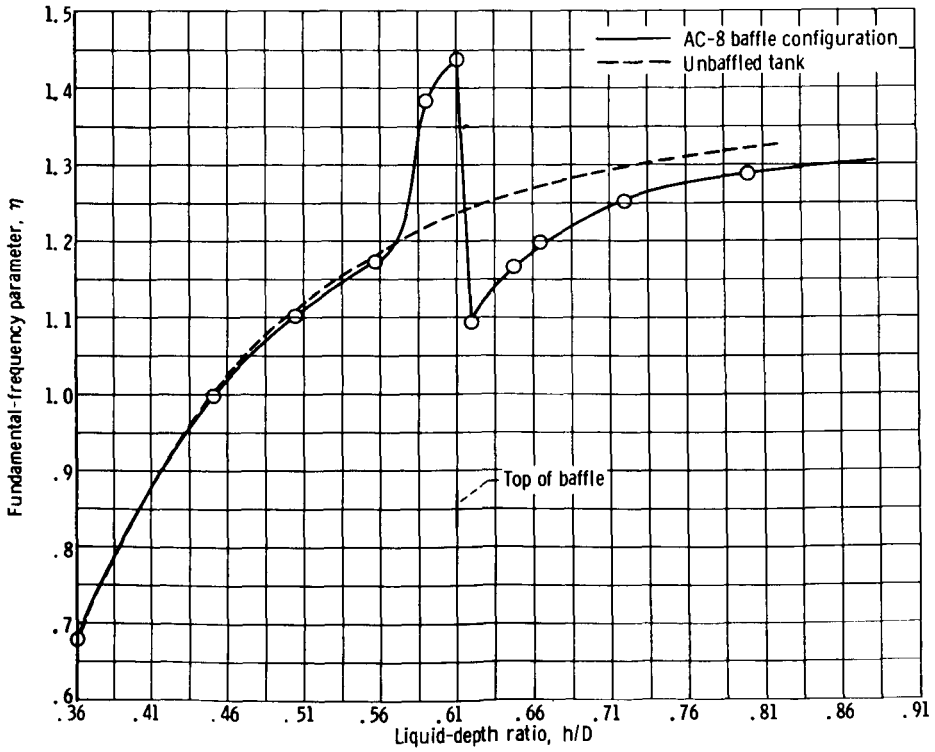

Figure 18. - Fundamental-frequency parameter for AC-8 baffle configuration.

approximately 1.3 to 54.8 percent higher than those obtained for the preliminary-design Centaur baffle configuration (fig. 6, pp. 11 and 12). This increase, as well as the additional slosh damping obtained for liquid levels just below the AC-8 baffle ($0.460 < h/D < 0.510$), was apparently due to the presence of the twelve vertical antiswirl baffles.

The minimum first-mode slosh-force parameters provided by the AC-8 baffle configuration (fig. 20) also occurred at liquid levels 0.01 tank diameter above the top of the baffle. The baffle was effective in reducing the minimum slosh forces to values slightly less than those obtained for the general Centaur baffle configuration (fig. 9, p. 17).

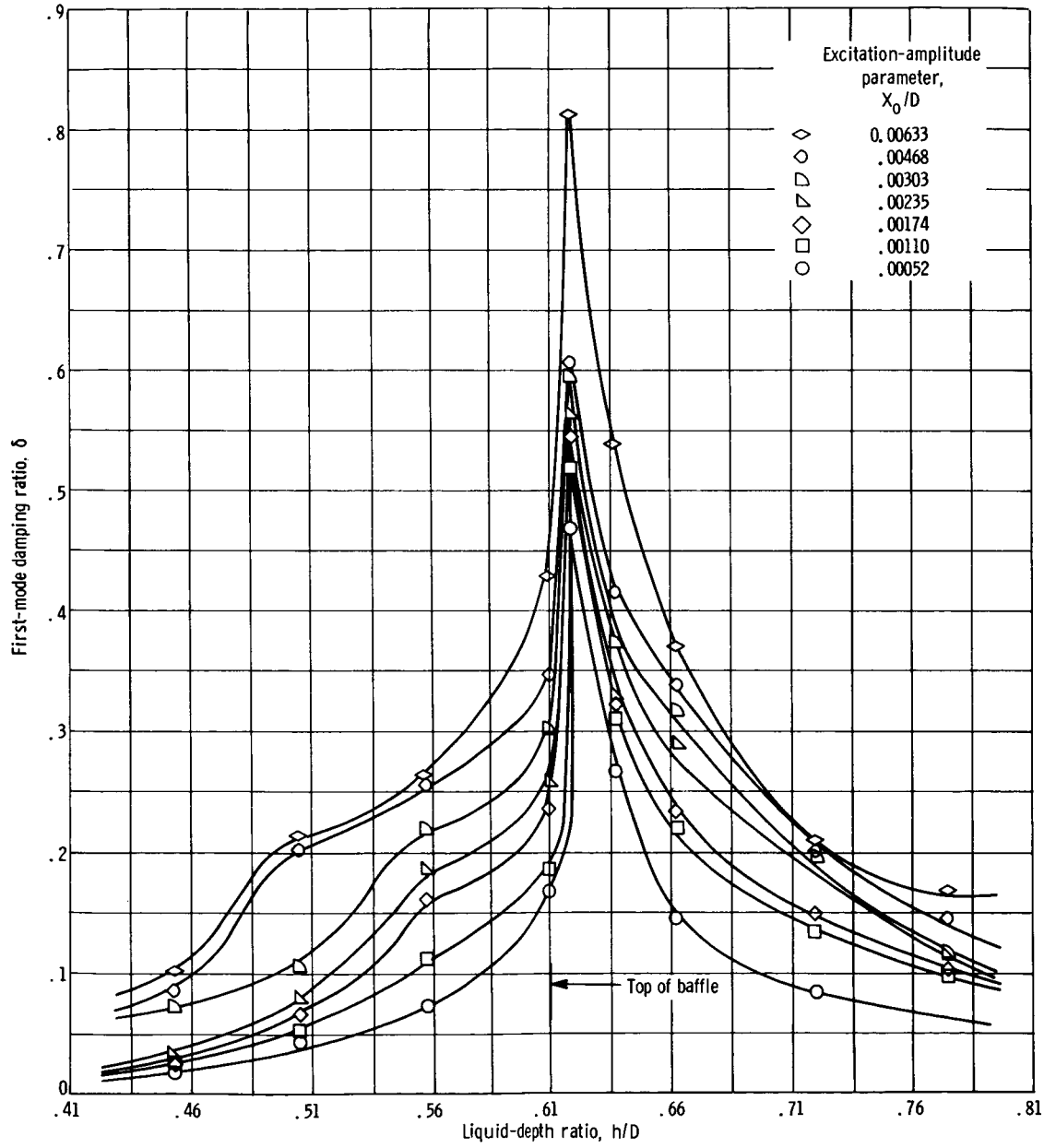

Figure 19. - First-mode damping ratio for AC-8 baffle configuration.

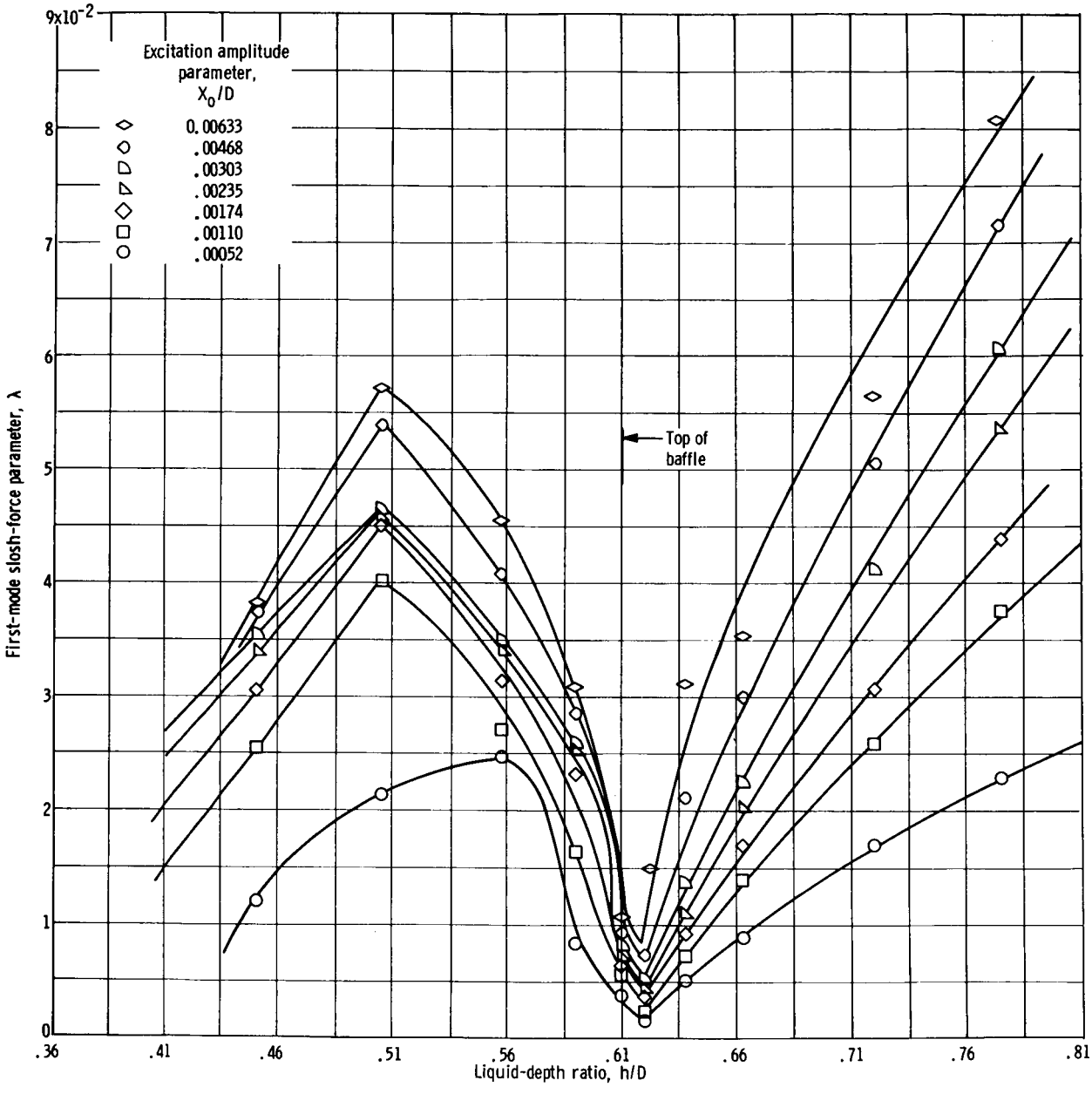

Figure 20. - First-mode slosh-force parameter for AC-8 baffle configuration.

REFERENCES

1. Silveira, Milton A.; Stephens, David G.; and Leonard, H. Wayne: An Experimental Investigation of the Damping of Liquid Oscillations in Cylindrical Tanks with Various Baffles. NASA TN D-715, 1961.

2. Bauer, Helmut F.: Fluid Oscillation in a Cylindrical Tank with Damping. Rep. No. DA-TR-4-58, Army Ballistic Missile Agency, Apr. 23, 1958.

3. Cole, Henry A., Jr.: On a Fundamental Damping Law for Fuel Sloshing. NASA TN D-3240, 1966.

4. Sumner, Irving E.; and Stofan, Andrew J.: An Experimental Investigation of the Viscous Damping of Liquid Sloshing in Spherical Tanks. NASA TN D-1991, 1963.

5. Sumner, Irving E.; Stofan, Andrew J.; and Shramo, Daniel J.: Experimental Sloshing Characteristics and a Mechanical Analogy of Liquid Sloshing in a Scale-Model Centaur Liquid Oxygen Tank. NASA TM X-999, 1964.

6. Lukens, David R.; Schmitt, Alfred F.; and Broucek, George T.: Approximate Transfer Functions for Flexible-Booster-and-Autopilot Analysis. Rep. No. AE 61-0198 (WADD TR-61-93), Convair-Astronautics, Apr. 1961.

7. Lomen, David O.: Liquid Propellant Sloshing Mobile Tanks of Arbitrary Shape. Rep. GD/A - DDE 64-061, General Dynamics/Astronautics, Oct. 15, 1964.

8. Lomen, David O.: Digital Analysis of Liquid Propellant Sloshing in Mobile Tanks with Rotational Symmetry. Rep. No. GD/A - DDE 64-062, General Dynamics/Astronautics, Nov. 30, 1964.

9. Garza, Luis R.; and Abramson, H. Norman: Measurements of Liquid Damping Provided by Ring Baffles in Cylindrical Tanks. Tech. Rep. No. 5 (NASA CR-52070), Southwest Research Inst., Apr. 1, 1963.

10. Miles, J. W.: Ring Damping of Free Surface Oscillations in a Circular Tank. J. Appl. Mech., vol. 25, no. 2, June 1958, pp. 274-276.

11. McCarty, John L.; Leonard, H. Wayne; and Walton, William C., Jr.: Experimental Investigation of the Natural Frequencies of Liquids in Toroidal Tanks. NASA TN D-531, 1960.

12. Sumner, Irving E.: Experimentally Determined Pendulum Analogy of Liquid Sloshing in Spherical and Oblate-Spheroidal Tanks. NASA TN D-2737, 1965.

13. Bauer, Helmut F.: Fluid Oscillations in the Containers of a Space Vehicle and Their Influence Upon Stability. NASA TR R-187, 1964.

"The aeronautical and space activities of the United States shall be conducted so as to contribute . . . to the expansion of human knowledge of phenomena in the atmosphere and space. The Administration shall provide for the widest practicable and appropriate dissemination of information concerning its activities and the results thereof."

—NATIONAL AERONAUTICS AND SPACE ACT OF 1958

NASA SCIENTIFIC AND TECHNICAL PUBLICATIONS

TECHNICAL REPORTS: Scientific and technical information considered important, complete, and a lasting contribution to existing knowledge.

TECHNICAL NOTES: Information less broad in scope but nevertheless of importance as a contribution to existing knowledge.

TECHNICAL MEMORANDUMS: Information receiving limited distribution because of preliminary data, security classification, or other reasons.

CONTRACTOR REPORTS: Technical information generated in connection with a NASA contract or grant and released under NASA auspices.

TECHNICAL TRANSLATIONS: Information published in a foreign language considered to merit NASA distribution in English.

TECHNICAL REPRINTS: Information derived from NASA activities and initially published in the form of journal articles.

SPECIAL PUBLICATIONS: Information derived from or of value to NASA activities but not necessarily reporting the results of individual NASA-programmed scientific efforts. Publications include conference proceedings, monographs, data compilations, handbooks, sourcebooks, and special bibliographies.

Details on the availability of these publications may be obtained from:

SCIENTIFIC AND TECHNICAL INFORMATION DIVISION

NATIONAL AERONAUTICS AND SPACE ADMINISTRATION

Washington, D.C. 20546